Custom Optics vs Modified COTS for Small Spacecraft : The Build vs. Rebuild Decision

Doug Sinclair
Sinclair Interplanetary
20 Maud St. Suite 200, Toronto, Ontario, M5V 2M5
dns@sinclairinterplanetary.com

John Enright, Tom Dzamba
Department of Aerospace Engineering, Ryerson University
350 Victoria St, Toronto, Ontario, M5B 2K3; 416-979-5000(x4174)
jenright@ryerson.ca

Thomas M. C. Sears
Sinclair Interplanetary
20 Maud St. Suite 200, Toronto, Ontario, M5V 2M5
tmcs@sinclairinterplanetary.com

ABSTRACT

This paper provides a comparative case study detailing parallel experiences with both a modified commercial off-the-shelf lens and a custom lens for small satellite applications. These lens designs were employed in two successive hardware generations of the ST-16 star tracker. The two designs are compared experimentally, measuring effective aperture, photometric efficiency, point-spread function and thermal stability. We show that opting for custom optical design can effectively remedy deficiencies in performance but often at the expense of technical and budgetary risks.

INTRODUCTION

Many small satellites incorporate optical cameras as part of the payload (remote sensing, astronomy, etc.) or the bus (star tracker, docking, etc.). The designer must select an appropriate lens suitable for their target application. Commercial Off-The-Shelf (COTS) lens assemblies are inexpensive, but require modifications to be suitable for flight. Custom lens development should get the hardware right the first time, but at a high cost. The authors have taken both paths: we have a modified COTS lens that we have flown many times, and we have recently completed the qualification of a custom lens assembly to replace it.

In this paper we discuss the performance of the COTS lens and of the custom lens. We show that some of the drawbacks of the COTS lens are not apparent upon reading the datasheet and are only discovered through testing. We also learn that building a custom lens for the first time carries terrible program risk.

Table 1: Detector properties

Part Number	ON Semiconductor MT9P031
Technology	CMOS Active Pixel
Resolution	2592 x 1944 pixels
Pixel Size	2.2 um square
Active Area	5.70 mm x 4.28 mm
Chief Ray Angle	7° at corner

SPECIFICATION

The Sinclair Interplanetary ST-16 series star trackers are the focus application for our study. The first generation star trackers (ST-16) used a COTS optical system and the second generation units (ST-16RT) employ the custom optical design [1]. The lenses are used to focus incident starlight onto a CMOS detector (see Table 1). Both designs share the same detector model. The 16 mm focal length is chosen to give a 15×21 degree full-angle field of view, which is enough to see the required three stars for the star tracking application.

Most stars detected by the star tracker are dim so improving the star tracker's sensitivity boosts its overall perfor-

Table 2: Lens specifications

Parameter	COTS Lens	Custom Lens
Part Number	Marshall Electronics V-4416.0-1.2-HR	Sinclair Interplanetary ST-16RT
Focal Length	16 mm	16 mm
f-number	$f/1.2$ (advertised) $f/1.68$ (measured)	$f/1.6$

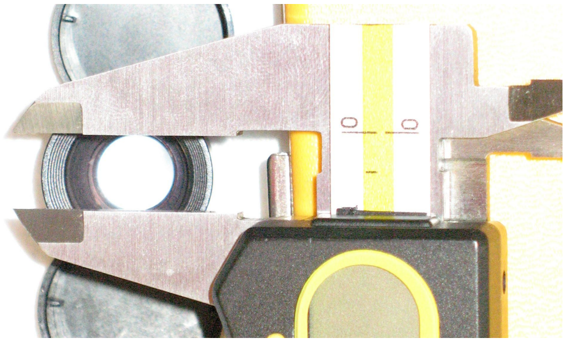

Figure 1: Measuring effective aperture of COTS lens with calipers and back-illumination.

Figure 2: Vignetting observed by viewing back-lit lens from off-angle (notice the bright circle is interrupted by the lens edge.)

mance. Several lens metrics affect the systems sensitivity. The f-number is a key lens specification, since it allows faint stars to be seen — i.e., lower f-numbers are typically more sensitive to dim illumination. High spatial resolution is also important, as it concentrates the starlight onto a smaller group of pixels and again assists in detection. Thermal stability is also desirable. Notwithstanding our focus on this particular application, we feel that the approach we took to examine the custom build decision is applicable to other types of optical payloads.

Our first key finding, shown in Table 2 is that the COTS lens falls far short of its datasheet $f/1.2$ specification. This result comes from the simple experiment shown in Figure 1. The effective aperture is 9.5 mm in diameter, which combined with a focal length of 16 mm gives:

$$f/\text{number} = \frac{f}{D} = 1.68 \qquad (1)$$

Looking into the COTS lens from off-axis (see Figure 2), gives direct evidence of vignetting. Although this figure exaggerates the effect — it is taken further away from the boresight than would be encountered in normal use — tests with the COTS lens demonstrated a measurable vignetting effect beginning at about 5° off-axis. This further reduces the effective aperture.

The custom lens was specified to have $f/1.6$ (slightly faster than the actual COTS lens) and no vignetting over a 7.5° half-angle cone.

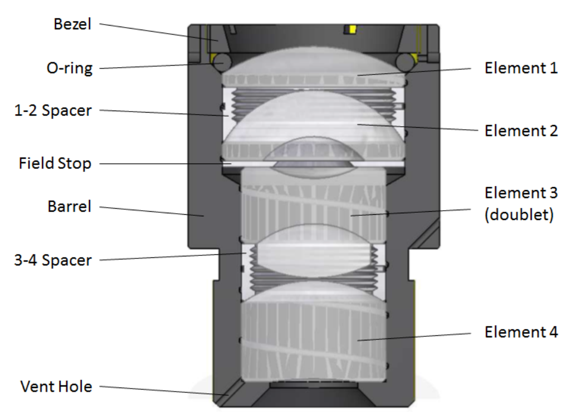

Figure 3: Cross-section view of custom lens.

MECHANICAL

Both the COTS and custom lenses have similar mechanical designs. An aluminum barrel serves as the primary structure, and is threaded at the base to screw into the camera body. The barrel has an internal cylindrical bore of varying diameters, larger at the top and stepping down to smaller at the bottom. The glass elements are loaded in from the top, and are constrained laterally by precision machining of the glass and metal diameters. Elements 3 and 4, and elements 1 and 2, are separated by machined aluminum spacers. Figure 3 shows the custom lens mechanical design.

Table 3: Lens diameters

Parameter	COTS Lens	Custom Lens
Element 1	17 mm	14.5 mm
Element 2	11.5 mm	14.5 mm
Element 3	9.4 mm	11.5 mm doublet
Element 4	8 mm	11.5 mm
Interface thread	M12x0.5	M16x0.5

The COTS lens presses element 2 and 3 together, using a layer of black paint at the interface as the field stop. The custom lens uses an aluminum field stop disk with a knife-edge to separate elements 2 and 3. A channel machined into the disk permits venting of the air in the pocket between the two elements which is trapped in the COTS design.

Both lenses use a threaded bezel at the front to retain the elements. In the COTS lens this bezel presses directly onto element 1. In the custom design an O-ring is squeezed between the bezel and the front glass. This is the key to the temperature stability of the custom lens. At high temperature the aluminum body expands faster than the glass, and the COTS lens loses all preload. In contrast, the custom lens uses the O-ring as a spring maintaining almost constant preload.

Table 3 shows the differences in diameters of the various lens features. The COTS lens uses an M12 interface thread for compatibility with many small cameras. This inherently limits the size of the rear elements. Even though the front element is large, giving the appearance of great aperture, the custom lens actually achieves greater effective aperture and far less vignetting due to its larger rear elements.

PHOTOMETRIC EFFICIENCY

The photometric efficiency of the lenses was measured by coupling the camera to an integrating sphere. This provides uniform illumination from all angles. The results are shown in Figure 4 where two features stand out. First, the custom lens has a greater brightness at the center of the image than the COTS lens. Second, the custom lens stays at essentially constant brightness out to an angle of 7.5° and then falls off sharply while the COTS lens brightness decays immediately either side of the boresight.

The improved numerical aperture and lack of vignetting contribute to these curves as previously discussed. Another key factor is the matching of the lens to the detector microlenses (Figure 5). CMOS active pixel sensors commonly use an array of microlenses to concentrate the

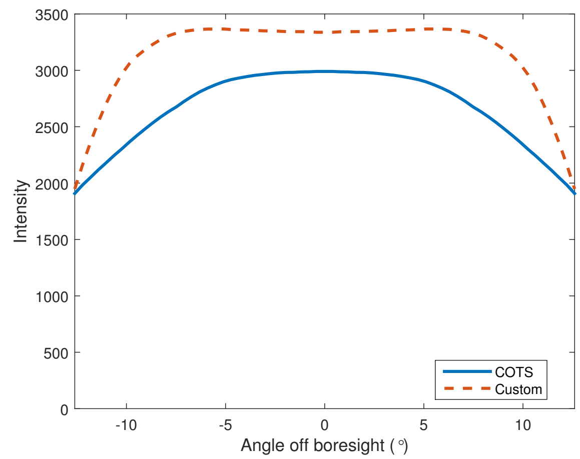

Figure 4: Comparative optical throughput of COTS vs custom lens.

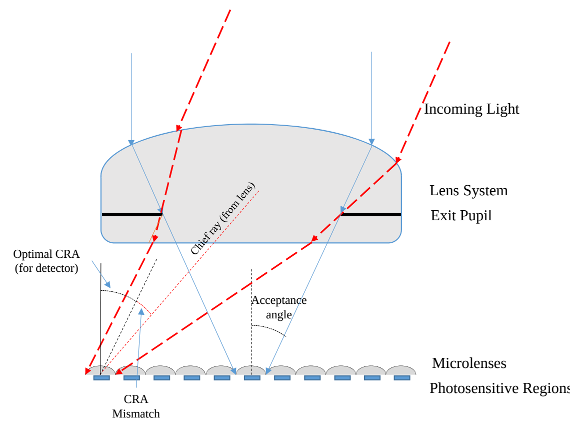

Figure 5: Schematic diagram showing the effect of microlens acceptance angle.

incoming light onto the photosensitive areas of the detector. This improves the effective fill factor of the detector by compensating for the area of the detector needed for non-photosensitive circuitry. Light from the system lens arrives at the microlenses at a range of different angles. If the ray incidence angle at the detector differs greatly from the designed chief ray angle (CRA), a significant fraction of the incoming light will be lost (the range of angles on either side of the CRA where the microlens offers good transmission efficiency is known as the acceptance angles). The location and dimensions of the exit pupil determine how well the lens system is matched to the detector microlenses.

The detector microlens array is designed for a 7° CRA (see Table 1). This is equivalent to requiring that the lens exit pupil be located 29 mm from the image plane. When this is done, as with the custom lens, most of the light that

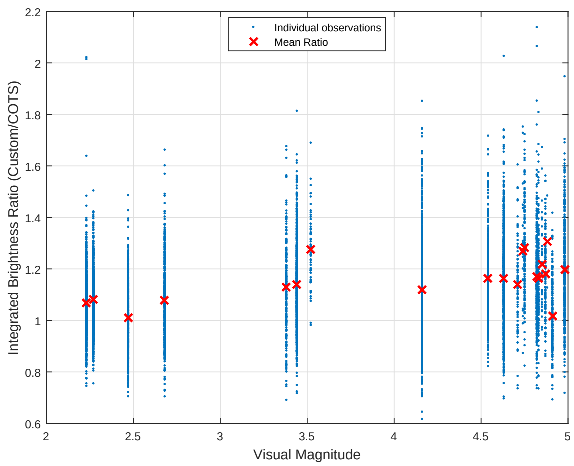

Figure 6: Comparison of star tracker detection sensitivity during night-sky tests.

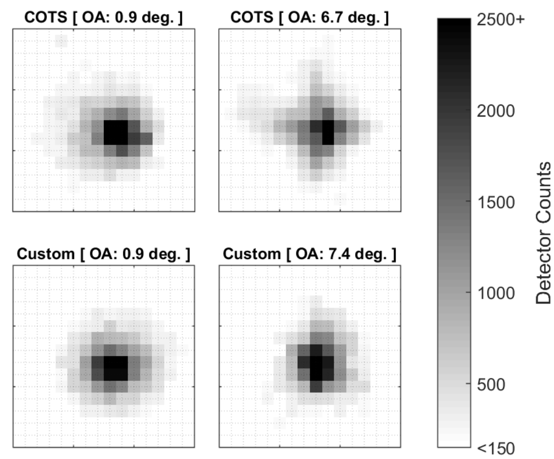

Figure 7: Comparison of point spread functions.

strikes the detector makes its way into the pixels. If the lens is not matched to the microlens array, as is almost certainly the case for the COTS lens, some of the light striking the detector is scattered off while other light hits non-sensitive areas of silicon.

The improved photometric efficiency at moderate angles (e.g. 5° from boresight) is key to the performance of a star tracker. This permits us to see faint stars over a greater solid angle. Figure 6 shows a comparison of the ratio between observed brightness in the COTS and custom lenses. These data were collected during a night-sky test in which two star trackers were mounted side-by-side, allowing simultaneous observations of the same stars. Both the individual ratios and the mean ratios are plotted on the graph. There is a fair amount of scatter in the plot, but the mean ratios are all greater than unity. The largest brightness improvements come from observations of dim stars (i.e., large visual magnitude).

POINT-SPREAD FUNCTION

One pixel on the star tracker detector spans an angle of 28 arcseconds. To reach the necessary accuracy, starlight must be spread over a number of pixels so that we can centroid the spot to sub-pixel precision. However, we do not want the spot to be too large or else faint stars will blend into the background. Adjusting the unit focus during manufacture can give some control over where the minimum blur radius lies in the FOV, but a lens that maintains consistent Point Spread Function (PSF) size across a wide range of off-axis angles is strongly desirable.

Figure 7 shows spots obtained from COTS and custom lenses. The star simulator used for these laboratory tests consists of a broadband fiber-coupled light source, a pinhole, and an off-axis parabolic telescope for collimation. The figures on the left are at an Offset Angle (OA) of 0.9°, and so are very close to the boresight. The figures on the right are close to the edge of the field of view. The custom lens retains circular spots across the whole field, while the COTS lens displays cross-shaped spots away from the boresight.

Table 4: Encircled energy comparison

Off-Axis Angle (°)	**85% radius (pixels)**	
	r_{COTS}	r_{Custom}
1	5.04	4.32
4	5.03	4.59
7	5.84	4.18

Data in Table 4 supports this result. The radius describes a circle that would contain 85% of the spot's energy. The custom lens maintains a smaller radius under all conditions, while the COTS lens shows a radius that increases at the edge of the field of view. Both of these radii are adequate for sub-pixel centroiding, but the smaller radius for the custom lens permits fainter stars to be seen.

THERMAL STABILITY

Analysis of some of the initial on-orbit data from the ST-16 using the COTS lens showed temperature-dependent boresight motion[2]. Although not catastrophic, this effect was undesirable and limited the utility of the sensor when high precision attitude measurements were required.

Subsequent analysis of the ST-16 construction suggested that some of the thermal deformations could be traced to two factors: 1) the detector/PCB mounting within the

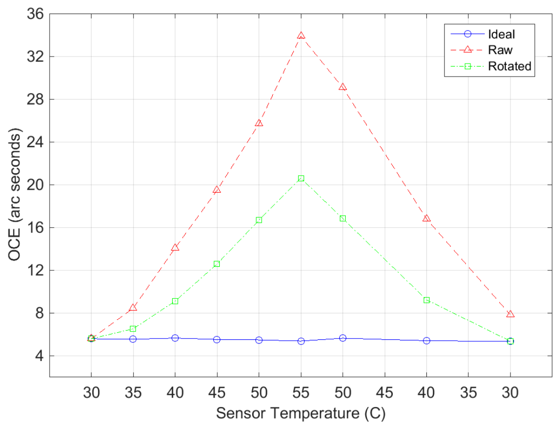

Figure 8: Effect of temperature on ST-16 calibration residuals (with COTS lens).

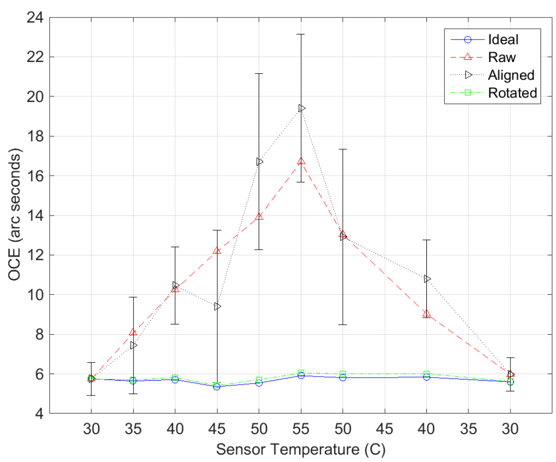

Figure 9: Effect of temperature on ST-16RT calibration residuals (with Custom lens).

chassis and 2) the thermal behaviour of the lens system itself. The former effect was corrected in the chassis redesign as part of the ST-16RT development, while improving the thermal behaviour of the lens systems was an additional motivating factor in opting for a custom lens design.

The custom lens cell thermal performance was simulated using the Zemax software. This took into account the thermal expansion of all of the materials, and the index of refraction changes of the various glasses. The dimensions and constraints were tuned by hand until the focal length was found to be essentially invariant with temperature.

Laboratory testing was used to confirm the thermal behaviours observed on orbit and in simulation. The apparatus consists of a three-axis gimbal rotating a heated platform on which the star tracker is mounted. A telescope projects the image of a single star at infinite distance, and the gimbal is moved to sweep this star across the sensor's field of view. Initial measurements made at room temperature allow us to calibrate a geometric model of the system's imaging behavior (see Enright, et al.[3] for details of the model). Additional measurements made over elevated temperatures allow us to determine the thermal sensitivity. Sensor performance is expressed in terms of the optical calibration error (OCE), σ_e, a measure of the RMS angular error from a set of true and measured star vectors.

Figure 8 shows the results from a COTS lens heated from 30°C to 55°C, and then cooled back to 30°C. The comparison of the room-temperature model with the data at subsequent temperatures (`raw`) shows a peak error of 34 arcseconds at 55°C. It also shows a hysteresis of approximately 2 arcseconds when the unit returns to 30°C. This peak error is large compared to the 10 arcsecond nominal performance of the sensor.

The rigid rotation data (`rotation`) shows the OCE when the sensor observations are updated with an optimum rotation at each temperature. This removes any bulk rotation in the measured star vectors and cancels the effect of secular boresight motion. There is no hysteresis in this curve, so we know that the system hysteresis comes from boresight rotation only. The peak OCE of 20 arcsecond at 55°C shows that while boresight rotation is significant, it is not the only source of error. There are clearly other optical effects, such as change of focal length.

Finally, the recalibrated data (`ideal`) shows the OCE when the calibration model is fully updated at each temperature. This is flat, showing that all of the changes with temperature can be accounted for in modeling parameters. There is no obvious noise increase due to detector dark current.

Figure 9 shows a similar set of test results from the custom lens. The `raw` data now peaks at 17 arcsecond, which is exactly half of the OCE of the COTS lens. Furthermore, the `rotated` data is now flat. This shows that all of the OCE is due to boresight rotation. The custom lens has no variation in focal length or other parameter with temperature.

The `aligned` curve shows the raw data, with the boresight vector updated from an observation of the optical cube mounted to the ST-16RT chassis. It has some noise, but it generally agrees with the raw data. This proves that the boresight vector motion is coming from the sensor itself, and that heated platform is not warping with temperature.

DESIGN DEFICIENCIES

Both the COTS and custom lenses had some serious deficiencies of design that had to be overcome before using them in space. In both cases, these flaws manifested themselves late in the program when flight hardware was almost ready to deliver. Fortunately, both were caught by Sinclair Interplanetary before launch.

COTS Lens: Preload

As discussed earlier, the COTS lens has no O-ring or other spring mechanism to maintain axial preload on the glass. Some lenses have a little preload from stored strain in the aluminum lens barrel, generated during factory assembly when the bezel is tightened and staked. However, this preload can disappear at high temperature as the aluminum expands faster than the glass.

Other lenses have no preload at all. The simple test for preload is to place a gloved finger on the center of the front glass and rotate. If the glass is free to spin in the lens cell then there is no preload. Lenses without preload will produce good images, but the optical parameters will vary with handling and temperature as the glass slides laterally.

After some experimentation we determined a simple procedure to ensure preload in these lenses. A small quantity of acetone is used to dissolve the staking on the lens bezel so that it can be rotated. The bezel is then torqued by hand to a snug position. Finally the bezel is re-staked, this time with two-part epoxy.

This problem was likely not of concern to the lens manufacturer, since in all conditions the lens does take adequate pictures. For its intended application as a security camera lens it is entirely adequate. It is only when attempting star tracking or other tasks requiring extreme geometric precision that it becomes limiting.

Custom Lens: Doublet Delamination

The custom lens uses a doublet in element 3 to give achromatic performance. The doublet is made from two different types of glass, cemented together with optical adhesive. The first iteration of the design chose glasses with large relative differences in coefficient of thermal expansion (> 3 ppm/C°) which lead to stress on the cement over temperature. The adhesive at the outer diameter of the bond experienced cohesive failure, fracturing into fine fern-like patterns (see Figure 10).

This issue was discovered very late in the qualification process, when candidate flight parts had already been manufactured. These are the risks that we take when specifying a custom lens design. There may be a hidden flaw in the engineering which only becomes apparent after extensive testing. The resulting redesign and remanufacture may take months as new glass is sourced, ground, polished and coated.

Figure 10: Delamination in the adhesive used in the element 3 doublet of the Custom lens.

Table 5: Lens Cost

Parameter	COTS Lens	Custom Lens
Non-Recurring Cost	$0	$100,000
Recurring Cost (Parts)	$40	$5,100
Recurring Cost (Labor)	$250	$0

COST

A comparison of custom and COTS lenses would not be complete without a discussion of cost. Table 5 shows an estimate of the non-recurring and recurring costs. The non-recurring costs are driven by the labour costs of the very expensive designers who determine the lens prescription, and then prepare the mechanical design for the lens cell and associated spacers and elements. Software license costs are also included in this amount. The recurring parts cost covers the purchase of a COTS lens, and the grinding, polishing, coating and assembling of custom glass together with machining and coating custom metal pieces.

CONCLUSION

The custom star tracker lens that we have built compares very favourably over the COTS lens. The increased photometric efficiency makes the whole scene brighter, especially around the edges. Additionally, the tighter point spread function makes star images sharper, further brightening the center of stars. The combination of these two effects makes it possible to see stars that are up to one magnitude dimmer than was previously possible with the COTS lens. This acts to improve overall system performance. In a sparse scene, seeing three stars instead of two is the difference between a successful star lock and failure. In a dense scene, seeing eight stars instead of five gives additional information to produce a more accurate attitude estimate.

The increased thermal stability of the custom lens is useful for those missions that will see large temperature variations across an orbit. The COTS lens sees thermal changes in many parameters, while the custom lens sees only a bulk rotation which is deterministic and can perhaps be calibrated out.

Both lenses have given us their share of headaches. The COTS lens required retorquing, while the custom lens has adhesive problems over temperature. Whichever path a program takes, whether optics will be purchased or fabricated, thorough qualification testing should be performed early to mitigate the schedule risks of late discoveries.

References

1. Enright J., Sinclair D., Dzamba T., "The Things You Can't Ignore: Evolving a Sub-Arcsecond Star Tracker," Proc. of the 26th AIAA/USU Conference on Small, vol. SSC12-X-7, Logan, Utah, 2012.

2. Dzamba T., Enright J., McVittie G., Sinclair D., Grant C., "Commissioning the S3S Nanosatellite Star Tracker," 61st International Astronautical Congress, vol. 6, pp. 4635–4649, Prague, Czech Republic, 2010.

3. Enright J., Jovanovic I., Vaz B., "On-Orbit Star Tracker Recalibration: A Case Study," IEEE Aerospace Conference, Big Sky, MT, 2015.